Macromolecules

Article

pubs.acs.org/Macromolecules

Effective Light-Harvesting Antennae Based on BODIPY-Tethered Cardo Polyfluorenes via Rapid Energy Transferring and Low Concentration Quenching

Hyeonuk Yeo, Kazuo Tanaka, and Yoshiki Chujo*

Department of Polymer Chemistry, Graduate School of Engineering, Kyoto University, Katsura, Nishikyo-ku, Kyoto 615-8510, Japan

Supporting Information

ABSTRACT: Light-harvesting antennae (LHA) were demonstrated using polyfluorenes (PFs) modified with borondipyrromethene (BODIPY) dyes tethered to the cardo structures. PFs work as a light absorber and an energy donor to the BODIPY units. The series of BODIPY-tethering PFs via the cardo carbon including homocardo PFs and alternative polymers with fluorene and the cardo fluorene were synthesized, and their optical properties were investigated. Initially, highly efficient energy transferring was observed from the PF main chains to the BODIPY unit (99%). It was found that PFs can work as an efficient light absorber because of the large molar extinction coefficient and cause the rapid energy transfer through the cardo structure. Next, from the comparison with the emission efficiency of the BODIPY units in the series of the synthetic polymers, the favorable position of the BODIPY units was obtained to avoid the concentration quenching: The alternative polymer with cardo fluorene and dialkyl-substituted fluorene showed the largest emission efficiency in this study. Finally, we received the effective LHA with the 9 times larger amplification efficiency compared to that of the unimolar BODIPY unit. The results from the computer modeling suggest that the positions of the BODIPY units via the cardo structure could play a significant role in the inhibition of aggregation and electronic coupling with the BODIPY units, leading to the suppression of concentration quenching. Here is presented the feasibility of the cardo structure in fluorene as a scaffold for designing advanced optical materials.

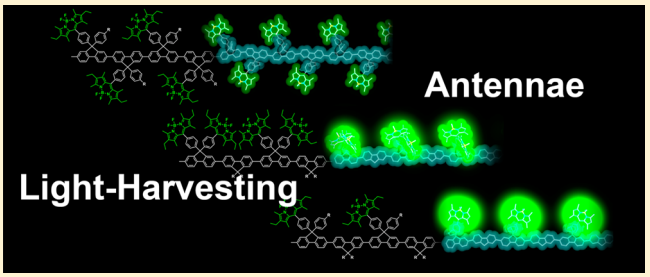

INTRODUCTION

Light-harvesting antennae (LHA), which can enhance the amount of light absorbing and transport the energy to a chromophore, are feasible for improving the efficiencies of solar cells or electroluminescence devices.[1,2] Because of the extremely high efficiency of the photosynthesis, many researchers have aimed to mimic the natural LHA systems or build new nanoarchitectures and molecular assemblies to close and overcome the efficiency of the natural ones.[3−5] On the construction of LHA systems, precise controls of assemblies and distributions between energy donors and acceptors to realize electronic communications with incorporated molecules are crucial.[6] To achieve the construction of these nanoassemblies with the functional molecules according to the preprogrammed design, one feasible strategy is using the conjugated polymers as a template.[7] By introducing the functional units into the polymer main chains and interacting them via the conjugation systems, the gathering of the light energy and the effective energy transferring can be expected.

We paid attention to the cardo polyfluorene (PFs) as a scaffold for constructing the functional assembly.[8] The PF is one of conventional optoelectronic polymeric materials because of the bright blue emission between 400 and 500 nm and the high hole-transport abilities. Because of these characteristics, PFs-based optical materials involving the LHA systems have been developed.[9] The tetrahedral bonding carbon (the 9-position of a fluorene) at the center of the cardo structures holds the substituted aromatic rings arranged three-dimensionally to the fluorene unit. Because of the steric hindrance of the bulky rings, the interchain and/or intrachain aggregations of the main chains are inhibited.[10] Consequently, unexpected changes in the emission properties such as red-shifting or self-quenching are highly suppressed.[10] Moreover, we have recently reported that the electronic coupling via the cardo structures hardly exist for the electronic properties of the PF main chains having the electron-donating and/or the electron-withdrawing groups at the aromatic rings of the cardo structures.[8] From these advantages of the cardo PF, we expected that the cardo PFs should be suitable scaffold to define the positions of donor and acceptor units on the polymer main chains and mediate the transferring of the excitation energy for achieving highly efficient LHA systems.

There are several previous works on the energy transferring involving the cardo PFs.[11] Xu and co-workers reported a series of the LHA involving fluorescence resonance energy transfer using the PF-based conjugated polymers as an energy donor.[12]

Received: January 3, 2013
Revised: March 3, 2013

dx.doi.org/10.1021/ma400015d | *Macromolecules* XXXX, XXX, XXX−XXX

Their systems were composed of a dye molecule as an energy acceptor in a mixture solution and could enhance the two-photon excitation fluorescence. In another study with the dye-tethered cardo PFs, effective energy transfer was observed through the cardo structures.[13] These results suggest the feasibility of the cardo PFs to fabricate the practical optoelectronic materials. On the other hand, although emission properties of dyes are generally spoiled when the dyes are gathered into local spaces, the influence of locations and positional relationships with dyes was hardly examined. This information should be necessary on the material design to avoid undesired annihilation process, called concentration quenching.[14] In other words, the degree of electronic interaction among dye molecules should be clarified schematically in the dye-tethered cardo PFs.

Herein, to gather the schematic information on the interaction of the dye molecules in the PFs, we prepared a series of the borondipyrromethene (BODIPY)-tethered PFs involving the cardo structures at various positions. From the evaluation of the efficiencies in each step of the LHA process with the synthetic polymers, the optimal positions of the dyes were explored. This is the first example, to the best of our knowledge, to present the guideline for constructing highly emissive materials based on the dye-tethered PFs.

EXPERIMENTAL SECTION

General. ^{1}H NMR, ^{13}C NMR, and ^{11}B NMR spectra were measured with a JEOL EX-400 (400 MHz for ^{1}H, 100 MHz for ^{13}C, and 128 MHz for ^{11}B) spectrometer. Coupling constants (J value) are reported in hertz. ^{1}H and ^{13}C NMR spectra used tetramethylsilane (TMS) as an internal standard. ^{11}B NMR spectra were referenced externally to $BF_3{\cdot}OEt_2$ (sealed capillary) in $CDCl_3$. The number-average molecular weight (M_n) and the molecular weight distribution [weight-average molecular weight/number-average molecular weight (M_w/M_n)] values of all polymers were estimated by size-exclusion chromatography (SEC) with a TOSOH G3000HXI system equipped with three consecutive polystyrene gel columns [TOSOH gels: α-4000, α-3000, and α-2500] and ultraviolet detector at 40 °C. The system was operated at a flow rate of 1.0 mL/min with THF as an eluent. Polystyrene standards were employed for the calibration. UV−vis spectra were recorded on a Shimadzu UV-3600 spectrophotometer. Fluorescence emission spectra were recorded on a HORIBA Jobin Yvon Fluoromax-4 spectrofluorometer, and the absolute quantum yield was calculated with the integrating sphere on the HORIBA Jobin Yvon Fluoromax-4 spectrofluorometer in chloroform. Fluorescence lifetime analysis was carried out on a HORIBA FluoreCube spectrofluorometer system; excitation at 375 nm was carried out using a UV diode laser (NanoLED-375L). Cyclic voltammetry (CV) spectra were recorded on a BAS ALS electrochemical analyzer model 600D.

Materials. Tetrahydrofuran (THF), diethyl ether (Et_2O), and triethylamine (Et_3N) were purified using a two-column solid-state purification system (Glasscontour System, Joerg Meyer, Irvine, CA). 9,9-Didodecylfluorene-2,7-diboronic acid and 2,4-dimethyl-3-ethyl-1*H*-pyrrole were obtained commercially and used without further purification. The monomers 4-(2,7-dibromo-9-(4-(octyloxy)phenyl)-9*H*-fluoren-9-yl)benzaldehyde and 4,4′-(2,7-dibromo-9*H*-fluorene-9,9-diyl)dibenzoic acid were prepared according to the literature.[8] All reaction was performed under an argon atmosphere.

Compound **1**. A flask charged with 100 mL of CH_2Cl_2 was degassed with Ar for 1 h, and 4-(2,7-dibromo-9-(4-(octyloxy)phenyl)-9*H*-fluoren-9-yl)benzaldehyde (2.57 g, 4.06 mmol), 2,4-dimethyl-3-ethyl-1*H*-pyrrole (1.00 g, 8.12 mmol), and three drops of trifluoroacetic acid (TFA) were placed. After the stirring for 2.5 h at room temperature, to the solution was added 2,3-dichloro-5,6-dicyano-*p*-benzoquinone (DDQ) (1.00 g, 4.41 mmol). After stirring for an additional 2 h at room temperature, NEt_3 (8 mL) and $BF_3{\cdot}OEt_2$ (8 mL) were added. After stirring overnight, the solution was evaporated. After flash chromatography on silica gel (10:1 = hexane:EtOAc, R_f = 0.45), recrystallization by hexane provided **1** (1.38 g, 1.52 mmol, 37%) as a red powder. ^{1}H NMR ($CDCl_3$, ppm): 7.60 (d, J = 8.0 Hz, 2H), 7.51 (d, J = 1.6 Hz, 2H), 7.48 (dd, J = 7.0 Hz, 1.6 Hz 2H), 7.26 (d, J = 8.6 Hz, 2H), 7.17 (d, J = 8.2 Hz, 2H), 7.06 (d, J = 8.8 Hz, 2H), 6.81 (d, J = 8.8 Hz, 2H), 3.92 (t, J = 6.5 Hz, 2H), 2.51 (s, 6H), 2.29 (q, J = 7.5 Hz, 4H), 1.80−1.71 (m, 2H), 1.48−1.39 (m, 2H), 1.38−1.21 (m, 14H), 0.97 (t, J = 7.4 Hz, 6H), 0.88 (t, J = 6.7 Hz, 3H). ^{13}C NMR ($CDCl_3$, ppm): 158.48, 153.75, 153.26, 145.94, 139.63, 138.24, 138.01, 135.35, 134.77, 132.85, 131.05, 130.71, 129.18, 128.90, 128.56, 128.46, 121.87, 121.70, 114.64, 68.04, 64.96, 31.80, 29.32, 29.24, 29.22, 26.64, 22.64, 17.07, 14.58, 14.07, 12.47, 11.62. ^{11}B NMR ($CDCl_3$, ppm): 0.78. HRMS (p-ESI) calcd for $C_{50}H_{53}BBr_2F_2N_2O$: m/z 906.2560; found: m/z 906.2577.

Compound **2**. The solution containing thionyl chloride (40 mL) was added to 4,4′-(2,7-dibromo-9*H*-fluorene-9,9-diyl)dibenzoic acid (4.18 g, 7.41 mmol) and was refluxed overnight, and then residual thionyl chloride was removed under vacuum. Dibenzoyl chloride was obtained as a white solid and used directly for the next reaction. Degassed CH_2Cl_2 (250 mL) and 2,4-dimethyl-3-ethyl-1*H*-pyrrole (3.65 g, 29.6 mmol) were mixed, and the resulting solution was refluxed for 3 days. After cooling to ambient temperature, NEt_3 (20 mL) and $BF_3{\cdot}OEt_2$ (30 mL) were sequentially added. After refluxing overnight, the reaction mixture was diluted with CH_2Cl_2 and extracted with H_2O and brine. After drying over $MgSO_4$, the products were concentrated. After flash chromatography on silica gel (8:1 = hexane:EtOAc, R_f = 0.4), the compound **2** (0.90 g, 0.83 mmol, 11%) was obtained as an orange powder after recrystallization with hexane/EtOAc. ^{1}H NMR ($CDCl_3$, ppm): 7.64 (d, J = 8.0 Hz, 2H), 7.53 (dd, J = 8.0 Hz, 1.7 Hz, 2H), 7.50 (d, J = 1.7 Hz, 2H), 7.30 (d, J = 8.2 Hz, 4H), 7.22 (d, J = 8.2 Hz, 4H), 2.52 (s, 6H), 2.29 (q, J = 7.6 Hz, 4H), 1.28 (s, 6H), 0.97 (t, J = 7.7 Hz, 6H). ^{13}C NMR ($CDCl_3$, ppm): 153.82, 152.67, 144.98, 139.24, 138.06, 135.11, 132.89, 131.34, 130.62, 128.96, 128.82, 128.27, 121.92, 121.90, 65.47, 17.01, 14.54, 12.44, 11.61. ^{11}B NMR ($CDCl_3$, ppm): 0.78. HRMS (p-MALDI) calcd for $C_{59}H_{58}B_2Br_2F_4N_4$: m/z 1080.315 10; found: m/z 1080.312 45.

Compound **3**. Benzoyl chloride (1.14 g, 8.12 mmol), 2,4-dimethyl-3-ethyl-1*H*-pyrrole (2.00 g, 16.2 mmol), and degassed CH_2Cl_2 (200 mL) were mixed, and the solution was refluxed for 2 days. After cooling to ambient temperature, NEt_3 (7 mL) and $BF_3{\cdot}OEt_2$ (14 mL) were sequentially added. The solution was concentrated by evaporation, and the crude products were treated with short chromatography on silica gel (3:1 = hexane:CH_2Cl_2, R_f = 0.7) for removing $BF_3{\cdot}OEt_2$. After flash chromatography on silica gel (9:1 = hexane:EtOAc, R_f = 0.5), compound **3** was obtained as an orange powder after recrystallization by hexane (0.40 g, 1.05 mmol, 13%). ^{1}H NMR ($CDCl_3$, ppm): 7.48 (s, 1H), 7.47 (d, J = 2.0 Hz, 2H), 7.28 (m, 2H), 2.53 (s, 6H), 2.29 (q, J = 7.6 Hz, 4H), 1.28 (s, 6H), 0.98 (t, J = 9.2 Hz, 6H). ^{13}C NMR ($CDCl_3$, ppm): 153.67, 140.19, 138.40, 135.81, 132.75, 130.78, 128.98, 128.70, 128.27, 17.06, 14.58, 12.45, 11.59. ^{11}B NMR ($CDCl_3$, ppm): 0.78. HRMS (p-ESI) calcd. for $C_{23}H_{27}BF_2N_2+H^+$: m/z 381.2308; found: m/z 381.2299.

Synthesis of Polymer ***P1***. The solution containing 1,5-cyclooctadiene (COD) (26.8 mg, 0.25 mmol), $Ni(COD)_2$ (68.0 mg, 0.25 mmol), and 2,2′-bipyridine (39.0 mg, 0.25 mmol) in 1 mL of anhydrous DMF was stirred at 60 °C for 30 min under an argon atmosphere, and then the monomer **1** (150 mg, 0.165 mmol) in 1 mL of anhydrous DMF was added. The reaction was stirred at 80 °C for 12 h in the dark, and then the products were reprecipitated several times with a small amount of chloroform into 150 mL of methanol. After Celite filtration to remove Ni, the red solid (134 mg, quant) was precipitated by pouring the chloroform solution of the product into 50 mL of methanol. ^{1}H NMR ($CDCl_3$, ppm): 7.80 (2H), 7.51 (4H), 7.39 (2H), 7.16 (4H), 6.77 (2H), 3.86 (2H), 2.50 (6H), 2.22 (4H), 1.71 (2H), 1.25 (16H), 0.89 (9H). ^{13}C NMR ($CDCl_3$, ppm): 158.21, 153.72, 152.39, 151.97, 147.26, 140.93, 139.73, 138.98, 137.97, 136.84, 134.34, 132.77, 130.71, 128.99, 128.72, 128.31, 126.89, 124.52, 120.59, 114.33, 67.94, 64.92, 31.77, 29.18, 26.03, 22.60, 17.02, 14.57, 14.04, 12.46, 11.58. ^{11}B NMR ($CDCl_3$, ppm): 0.78.

dx.doi.org/10.1021/ma400015d | *Macromolecules* XXXX, XXX, XXX−XXX

Scheme 1. Synthesis of the Monomers[a]

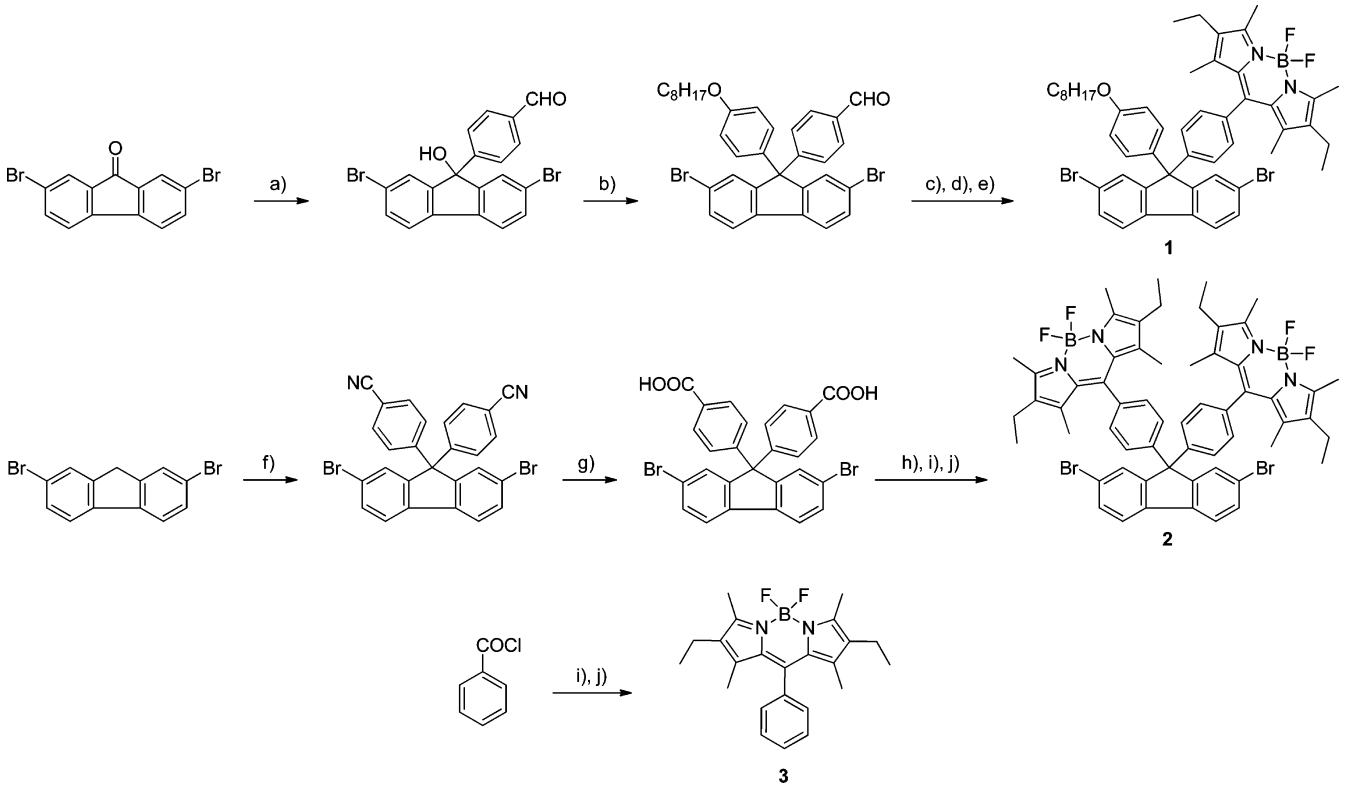

[a]Reagents and conditions: (a) Mg, 4-bromobenzaldehyde diethyl acetal, in THF, rt to reflux overnight and 2 N HCl(aq) 3 h; (b) *n*-octyl phenyl ether, CF_3SO_3H, in dioxane, 70 °C, 5 h; (c) 2,4-dimethyl-3-ethyl-1*H*-pyrrole, TFA, in CH_2Cl_2, rt, 3 h; (d) DDQ, 3 h; (e) NEt_3, $BF_3{\cdot}OEt_2$, overnight; (f) 4-fluorobenzonitrile, 18-crown-6, K_2CO_3, in DMF and toluene, 140 °C, overnight; (g) KOH, EtOH, H_2O, reflux, 5 days; (h) $SOCl_2$, reflux, 8 days; (i) 2,4-dimethyl-3-ethyl-1*H*-pyrrole, in CH_2Cl_2, reflux, 2 days; (j) NEt_3, $BF_3{\cdot}OEt_2$, reflux, overnight.

Synthesis of Polymer ***P2***. The solution containing tris(dibenzylideneacetone)dipalladium(0) ($Pd_2(dba)_3$) (4 mg, 0.004 mmol), 2-dicyclohexylphosphino-2′,6′-dimethoxybiphenyl (S-Phos) (7 mg, 0.017 mmol), cesium carbonate (Cs_2CO_3) (0.40 g, 1.23 mmol), **1** (150 mg, 0.165 mmol), and 9,9-didodecylfluorene-2,7-diboronic acid (97.7 mg, 0.165 mmol) in 1.5 mL of toluene and 1 mL of H_2O was stirred at 90 °C for 2 days under an argon atmosphere. The orange solid (188 mg, 91%) was precipitated by pouring the chloroform solution of the product into 50 mL of methanol twice. ^{1}H NMR ($CDCl_3$, ppm): 7.90 (2H), 7.68 (6H), 7.51 (6H), 7.25 (4H), 6.82 (2H), 3.90 (2H), 2.52 (6H), 2.27 (4H), 2.00 (2H), 1.74 (2H), 1.18 (m, 58H), 0.97 (6H), 0.83 (9H). ^{13}C NMR ($CDCl_3$, ppm): 158.19, 153.70, 152.56, 151.73, 147.47, 141.86, 141.42, 140.02, 138.92, 138.12, 134.24, 132.76, 130.81, 129.18, 128.92, 128.30, 127.02, 126.19, 124.68, 121.45, 120.54, 119.95, 114.40, 67.97, 64.96, 55.25, 40.37, 31.89, 31.79, 30.06, 29.60, 29.31, 29.21, 26.06, 23.91, 22.65, 22.62, 17.09, 14.64, 14.09, 14.06, 12.47, 11.70. ^{11}B NMR ($CDCl_3$, ppm): 0.78.

Synthesis of Polymer ***P3***. Similarly to the preparation of **P2**, the polymer **P3** was prepared with the monomer **2** (76 mg, 0.07 mmol) and 9,9-didodecylfluorene-2,7-diboronic acid (41.5 mg, 0.07 mmol) in the presence of $Pd_2(dba)_3$ (1 mg, 0.001 mmol), S-Phos (3 mg, 0.007 mmol), and Cs_2CO_3 (0.40 g, 1.23 mmol) as a red solid (105 mg, quant). ^{1}H NMR ($CDCl_3$, ppm): 7.95 (2H), 7.76 (4H), 7.69 (4H), 7.54 (2H), 7.48 (6H), 7.26 (2H), 2.52 (12H), 2.26 (8H), 2.01 (4H), 1.34 (12H), 1.13 (36H), 0.95 (16H), 0.82 (6H). ^{13}C NMR ($CDCl_3$, ppm): 153.86, 152.00, 151.81, 146.60, 141.58, 140.35, 140.05, 139.61, 139.04, 137.98, 136.79, 134.65, 132.84, 130.74, 128.68, 128.63, 127.41, 126.26, 124.62, 121.53, 121.22, 120.72, 119.99, 65.54, 55.25, 55.12, 40.32, 40.17, 31.87, 30.49, 30.04, 29.65, 29.59, 29.30, 28.94, 23.96, 22.63, 17.07, 14.62, 14.07, 12.48, 11.76. ^{11}B NMR ($CDCl_3$, ppm): 0.78.

RESULTS AND DISCUSSION

Synthesis of the Monomers. Because of strong emission intensity, low environmental dependency of optical properties, and high stability to photodegradation, BODIPY can be used as a conventional fluorophore for emissive materials and biomarkers.[15,16] The monomers containing the cardo structures with the single BODIPY and octyloxyphenyl group, **1**, and with the dual BODIPYs, **2**, were synthesized (Scheme 1). The dibromofluorene monomers **1** and **2** were obtained according to the previous reports using 2,7-dibromofluorenone and 2,7-dibromofluorene as a starting material, respectively.[8] We also prepared the compound **3** as a free BODIPY dye. All monomers were characterized by ^{1}H, ^{13}C, and ^{11}B NMR spectroscopies and mass measurements. In ^{11}B NMR spectra using $BF_3{\cdot}OEt_2$ as a standard, the products showed the peaks at 0.78 ppm assigned as a tetracoordinate boron. From these data, we concluded that the BODIPY units were constructed.

Synthesis of the Polymers. The polymerizations with the dibromo monomers **1** via Yamamoto coupling and with the dibromo monomers **1**, **2** and 9,9-didodecylfluorene diboronic acid via Suzuki−Miyaura coupling were executed as shown in Scheme 2. **P1** and **P3** have same number of the BODIPY unit per a fluorene unit but different positions. **P2** has one BODIPY unit per two fluorene units. To remove the metal species originated from the catalyst thoroughly, the Celite filtration for **P1** and the following reprecipitation from methanol were repeated twice. The solubility in conventional organic solvents seemed to be improved by introducing the cardo structures to the polyfluorene main chains. The number-average molecular

dx.doi.org/10.1021/ma400015d | *Macromolecules* XXXX, XXX, XXX−XXX

Scheme 2. Synthesis of the Polymers[a]

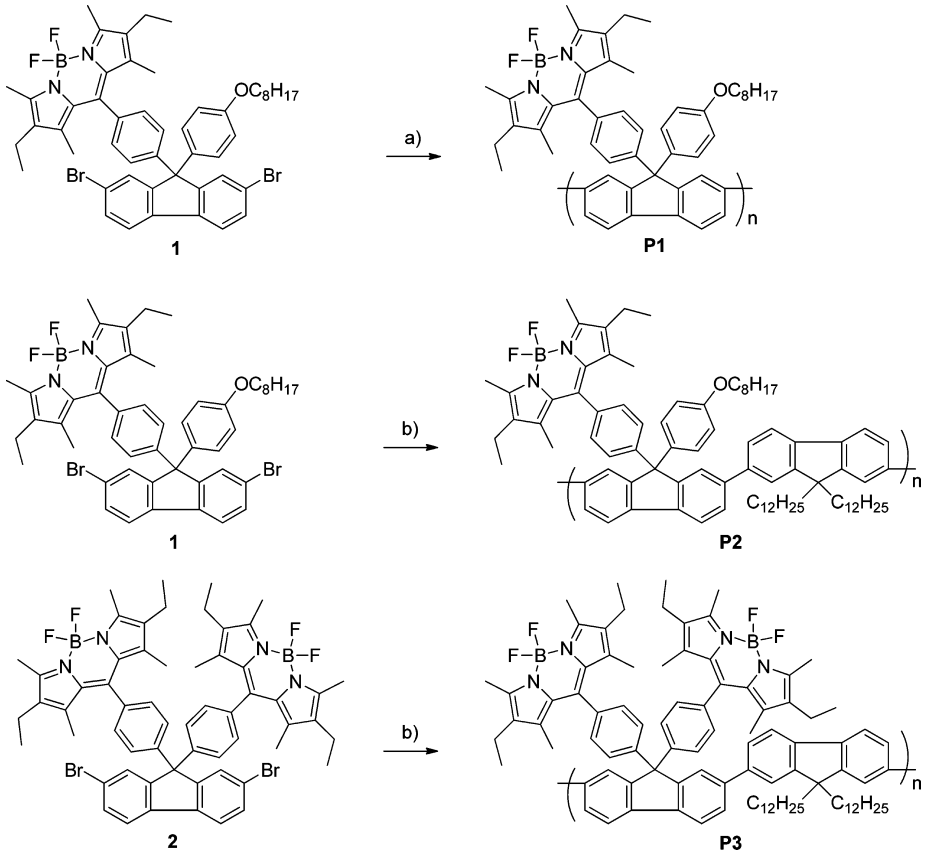

[a]Reagents and conditions: (a) $Ni(COD)_2$, COD, 2,2-bpy, in DMF, 12 h; (b) 9,9-didodecylfluorene-2,7-diboronic acid, $Pd_2(dba)_3$, S-Phos, Cs_2CO_3, toluene, H_2O, 2 days.

weights (M_n) and the molecular weight distributions (M_w/M_n) of the polymers, measured by the size-exclusion chromatography (SEC) in tetrahydrofuran (THF) toward polystyrene standards were from 5500 to 7000 with 2.1 to 3.7, respectively (Table 1). The synthesized polymers have longer chain lengths

Table 1. Polymerization Results

polymer	yield (%)[a]	M_n[b]	M_w/M_n[b]	DP
P1	quant	6200	3.95	8.3
P2	91	7000	2.30	11.2
P3	quant	5500	2.10	7.7

[a]Isolated yields after precipitation. [b]Estimated by size-exclusion chromatography (SEC) based on polystyrene standards in chloroform. [c]Degree of polymerization estimated by number-average molecular weight.

(**P3**: DP = 7.7) than the effective conjugation length at the excited states (ca. 5) in polyfluorene.[17] These results suggest that the influence of the polymer ends should be negligible on the optical properties as LHA. In addition, the data for structural analysis by ^1H, ^{13}C, and ^{11}B NMR corresponded to those of the monomers. Thus, we concluded that the polymers should possess the expected chemical structures as we designed.

Absorption Spectra of the Polymers. The optical properties of the polymers were initially investigated by UV–vis absorption in chloroform (Figure 1). The influence of the BODIPY units on the electronic properties of the main chains was examined. We prepared the mixture solutions named as

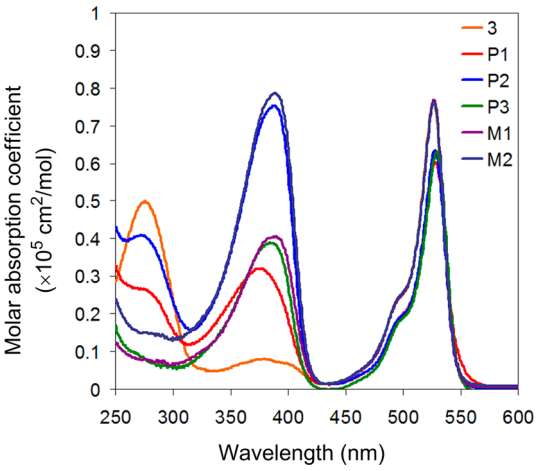

Figure 1. UV–vis spectra of the polymers and the model compounds in chloroform (1.0×10^{-5} M).

M1 containing 9,9-dioctylpolyfluorene (PFO, M_n = 18 500, PDI = 4.2, fluorene unit = 1.0×10^{-5} M) and **3** (1.0×10^{-5} M) as a comparison to **P1** and **P3**. **M2** containing PFO (fluorene unit = 2.0×10^{-5} M) and **3** (1.0×10^{-5} M) was also prepared for the comparison to **P2**. All measurements were executed with the samples containing 1.0×10^{-5} M of the BODIPY unit. The results from the absorption and emission spectra are summarized in Table 2. The unimolecular BODIPY **3** exhibited the strong and sharp absorption peak at 527 nm. Correspond-

dx.doi.org/10.1021/ma400015d | Macromolecules XXXX, XXX, XXX–XXX

Table 2. Photophysical Properties of the Polymers in Chloroform Solution

compd	$\lambda_{abs,max}$/nm[a]	$\lambda_{PL,max}$/nm[b]	Φ_{PL}[c]	$I_{PL,max}$[d]	Φ_{DA}[e]	$E_{eff,\Phi}$[f]	$E_{eff,I}$[g]	τ/ns[h]	χ^2[h]	E_{LHA}[i]
3	377 (8100), 527 (76500)	538	0.68	1.29				4.99	1.013	1.0
M1	388 (40400), 527 (76700)	416, 539		1.31						
M2	388 (78700), 527 (76200)	416, 538		1.30						
P1	377 (32000), 528 (60300)	539	0.46	0.46	0.001	0.999	0.995	4.21	1.123	1.7
P2	387 (75300), 527 (63500)	539	0.80	1.00	0.002	0.997	0.997	4.20	1.035	8.9
P3	383 (38900), 529 (63000)	539	0.72	0.74	0.014	0.981	0.998	3.96	1.013	3.9

[a]Evaluated in chloroform (1.0×10^{-5} M) (molar extinction coefficient). [b]Excited at 380 nm in chloroform (1.0×10^{-7} M). [c]Absolute quantum yield. [d]Fluorescence intensity of emission maxima excited at 525 nm. [e]Absolute quantum yield of the PF main chain. [f]Energy transfer efficiency calculated by quantum yield. [g]Energy transfer efficiency calculated by emission intensity at 420 nm. [h]Photoluminescence lifetimes of the polymers on emission wavelength 540 nm in chloroform (1.0×10^{-7} M). [i]LHA efficiency compared to **3**.

ingly, the polymers **P1**–**P3** showed the strong absorption peak at 527 nm. In absorption regions from 330 to 420 nm, **P1** and **P3** possessing a single fluorene unit per a single BODIPY unit showed similar levels of the molar extinction coefficient to PFO. Moreover, **P2** possessing two fluorene units per a single BODIPY unit exhibited the twice-larger molar extinction coefficient than that of PFO. These results mean that the electronic properties of the BODIPY units tethered to the polymers should be similar to that of a free BODIPY dye in the solution. In particular, it should be mentioned that the BODIPY units should be electronically independent of the polymer main chains as well as adjacent BODIPY units as representatively observed from **P3**. Accordingly, it is suggested that the intrinsic optical properties of BODIPYs and PF main chains can be observed from the synthesized polymers. These results can be explained by our previous findings that the cardo structure plays a role in inhibiting electronic couplings between the main chains and the side chains.[8] In contrast, **P1** provided red-shifted optical edge. It is assumed that the BODIPY units could form the stacking structure. The electronic structure of **P1** is discussed in the emission spectra.

The absorption spectra of the polymers were measured with the polymer films (Figure S1 and Table S1). The thin films were cast on the quartz plate by the spin-coating method with the chloroform solutions (1.0 mg/mL) of the polymers. Slightly red-shifted peaks were obtained from the spectra comparing with those from the solutions. These data imply that the isolation effect owing to the cardo structure could be received even in the condensed state such as in the film.

Emission Properties of the Polymers. The emission properties and the LHA efficiencies of **P1**, **P2**, and **P3** were evaluated in the chloroform solutions (Figure 2). The LHA efficiency was calculated from the ratios of the emission intensities toward that from **3** with the excitation light at 380 nm. The results are listed in Table 2. Significantly, it was found that **P2** and **P3** can work as a LHA with 8.9 and 3.9 times larger efficiencies than that of **3**. Even from the polymer **P1** in which the BODIPY units could form the aggregation, 1.7 times stronger emission than that of **3** was observed with the peak at 540 nm. The samples were prepared with the same concentrations of the BODIPY unit. It means that in the sample of **P2** the concentration of the PF main chains, light absorber, is 2-fold larger than that of **P3**. Therefore, the actual LHA value of **P3** calculated from the PF standard concentration should be similarly large value with that of **P2**. In summary, it can be claimed that the synthesized polymers should be efficient LHA.

The LHA efficiencies of the polymers were also measured in the film states (Figure 3). Generally, because of the strong

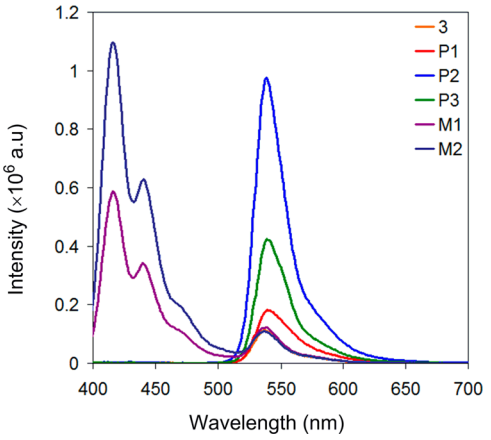

Figure 2. Photoluminescence spectra of the polymers in chloroform (1.0×10^{-7} M, excitation wavelength 380 nm).

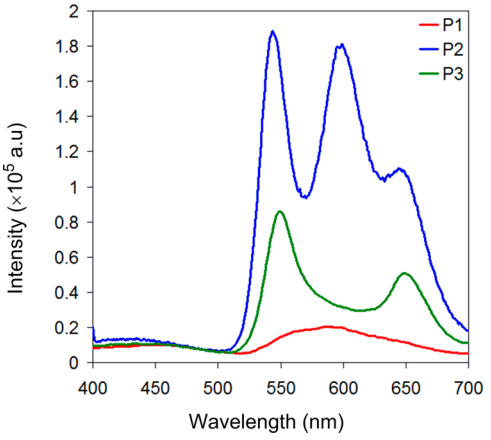

Figure 3. Photoluminescence spectra of the polymers in the film states (excitation wavelength 380 nm).

aggregation ability of BODIPY dyes, the emission drastically decreased in the solid states because of concentration quenching.[14] Indeed, the unimolecular BODIPY **3** showed no emission. On the other hand, the polymers **P2** and **P3** gave strong fluorescence emissions. These data indicate that the cardo PFs-based LHA systems should be valid for the practical usages as a device. The weak emission from **P1** can be explained by the aggregation formation similarly as observed in the solution state. It should be mentioned that the synthetic polymers have good processability similarly as PFs. These advantages as a material involving optical properties in the film states could be feasible for the application to practical devices.

dx.doi.org/10.1021/ma400015d | Macromolecules XXXX, XXX, XXX–XXX

Chart 1. Schematic Diagram for Energy Transferring

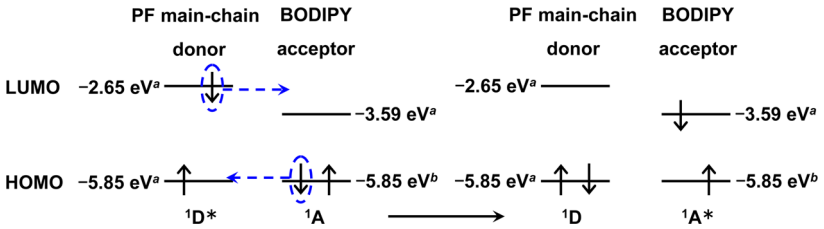

[a]Determined from cyclic voltammograms. [b]Calculated from the onsets of the polymers in the absorption spectra.

To investigate the photochemical process on the LHA, the spectra were analyzed in further detail. Initially, the polymers and models were dissolved in chloroform, and the photoluminescence spectra were obtained with the excitation light at 380 nm corresponding to absorption maxima of the PFs (Figure 2). In the emission region from 400 to 500 nm of the PFs, **M1** and **M2** showed similar spectra with the peaks at 420, 445, and 470 nm assigned as the 0−0, 0−1, and 0−2 intrachain singlet transition originated from PFO.[18] In contrast, the emission peaks originated from the PFs main chain were not observed in all polymers, but strong emission was obtained with the peak at 540 nm assigned as the fluorescence of BODIPY. Furthermore, the excitation spectra of the polymers were measured with the detection wavelength at 540 nm (Figure S2). The spectra were normalized by the peak top of BODIPY emissions. The peak positions showed good agreements with those in UV spectra. These data represent that efficient energy transfer from the PF main chains to the BODIPY units should occur through the cardo structures in the polymers. The energy transfer efficiencies were calculated according to the eq 1,[19] and the values are listed in Table 2:

$$E_{\mathrm{eff}} = (1 - I_{\mathrm{DA}}/I_{\mathrm{D}}) = (1 - \tau_{\mathrm{DA}}/\tau_{\mathrm{D}}) = (1 - \Phi_{\mathrm{DA}}/\Phi_{\mathrm{D}}) \quad (1)$$

where I_{DA} is a fluorescence intensity of donor in the presence of acceptor and I_{D} in the absence of acceptor, τ_{DA} is a fluorescence lifetime of donor in the presence of acceptor and τ_{D} in the absence of acceptor, and Φ_{DA} is a quantum yield of donor in the presence of acceptor and Φ_{D} in the absence of acceptor. All polymers indicated energy transfer efficiencies over 0.99 from the PF main chain to the BODIPY units. According to the energy levels of the PF and the BODIPY unit determined from optical and electrochemical measurements, the proposed mechanism on the energy transfer is illustrated in Chart 1. Surprisingly, although the electronic coupling via the cardo structure is very few, the energy transfer can proceed with high efficiency in the synthetic polymers. To gather the kinetics of the energy transfer in the polymers, the fluorescence lifetimes were measured. Because of too rapid process, the energy transfer rates from the PFs to the BODIPY units were not determined (<100 ps). These results imply the efficient energy transfer could occur.

In general, to receive highly emissive polymers, it is necessary to avoid the concentration quenching induced by the accumulation of chromophores.[10] To evaluate the degree of the emission properties of the BODIPY units in the polymers, we compared the photoluminescence quantum yields (QY) of these polymers. Initially, the quantum yields through the total process from the light absorption at the PF main chains to the emission from the BODIPY unit were calculated. By using the integration sphere, the absolute values were determined with the excitation light at 380 nm. The alternative polymer **P2** showed the highest QY value of the samples (Φ_{PL} = 0.80). Interestingly, the polymer **P3** that has the same backbone structure, but the intermolecular distances between the BODIPY units are much closer than those in **P2** presented similar degree of the QY value (Φ_{PL} = 0.72). In particular, the BODIPY units in these polymers showed higher QY values than that of **3**. Thermal quenching path could be suppressed by tethering the BODIPY unit to polymer chains via the rigid cardo structures. The smaller value obtained from the polymer **P1** than that of **3** implies the aggregation-induced quenching of the emission. Next, to evaluate the favorable position of the BODIPY unit for improving the emission efficiency, the photoluminescence spectra were obtained with the excitation light at 525 nm (Figure 4). From the emission intensities at the peak tops, the degree of the concentration quenching was evaluated as a relative value (Table 2). The BODIPY units in the polymer **P2** showed the largest value of the polymers. Notably, similarly as the QY values, the concentration quenching of the BODIPY units in the polymer **P3** was efficiently suppressed. These data clearly indicate that the cardo structure should play an important role in the preservation of the intrinsic properties of dyes.

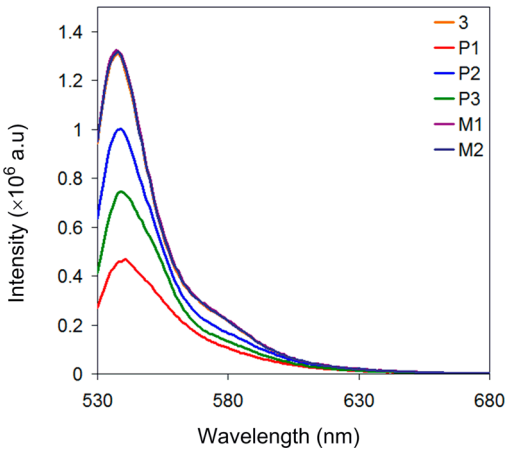

Figure 4. Photoluminescence spectra of the polymers in chloroform (1.0×10^{-7} M, excitation wavelength 525 nm).

Molecular Orbital Calculations. To understand a quenching phenomenon observed from **P1**, we employed the theoretical calculation for the models of the polymers using density-functional theory (DFT) at the B3LYP/6-31G(d)//B3LYP/6-31G(d) (Figure S4). The models of the polymers have the two or three repeat units, substituting alkyl chains to methyl groups for simplifying calculation. It was found that intramolecular dimer of the nearby BODIPY units could be

dx.doi.org/10.1021/ma400015d | *Macromolecules* XXXX, XXX, XXX−XXX

formed on the ground states in the **P1** model. On the other hand, each BODIPY unit hardly shows the interaction in the **P2** and **P3** models. It is known that the fluorescence emission from BODIPY dyes can be drastically quenched by the aggregation.[14] Thereby, the decrease of the emission intensity could be observed from **P1**. In contrast, in the **P3** model, plane angles of two BODIPY units are ∼120°, meaning little interaction between two BODIPYs on a cardo structure. These data suggest that the rigid and the orthogonal structure of the cardo should be favorable not only to avoid the concentration quenching of the dyes but also to accumulate the emissive dyes without unexpected changes in the electronic properties.

■ CONCLUSION

We present the first example to offer the schematic information on the changes of optical properties of the dyes depending on the location at the PF main chains. Considering the experimental results described here, we summarize that three significant advantages on the usages of the cardo structure involving PFs as a scaffold: (i) Large light absorption and effective energy transfer can be obtained. (ii) The intrinsic property of the dye can be observed after conjugation with the cardo PFs. (iii) The desired optical properties can be received in the film state. Finally, highly effective LHA systems were realized based on the BODIPY-tethered cardo PFs. Advanced LHA systems based on our design concept for higher efficiency or diverse light wavelength of absorption and emission are promised to be realized by modulating the location, the numbers, and the type of chromophores. In addition, further applications are in progress to utilize the cardo fluorene as a scaffold for constructing highly functional optical materials.

■ ASSOCIATED CONTENT

Ⓢ Supporting Information

Figures S1−S23 and Table S1. This material is available free of charge via the Internet at http://pubs.acs.org.

■ AUTHOR INFORMATION

Corresponding Author

*E-mail chujo@chujo.synchem.kyoto-u.ac.jp; Fax +81-75-383-2605; Ph +81-75-383-2604.

Notes

The authors declare no competing financial interest.

■ REFERENCES

(1) (a) Chen, C.-Y.; Wu, S.-J.; Li, J.-Y.; Wu, C.-G.; Chen, J.-G.; Ho, K.-C. *Adv. Mater.* **2007**, *19*, 3888−3891. (b) Hasobe, T.; Hattori, S.; Kamat, P. V.; Wada, Y.; Fukuzumi, S. *J. Mater. Chem.* **2005**, *15*, 372−380. (c) Warnan, J.; Pellegrin, Y.; Blart, E.; Odobel, F. *Chem. Commun.* **2012**, *48*, 675−677. (d) Li, Y.; Bian, Y.; Yan, M.; Thapaliya, P. S.; Johns, D.; Yan, X.; Galipeau, D.; Jiang, J. *J. Mater. Chem.* **2011**, *21*, 11131−11141.

(2) (a) Brovelli, S.; Meinardi, F.; Winroth, G.; Fenwick, O.; Sforazzini, G.; Frampton, M. J.; Zalewski, L.; Levitt, J. A.; Marinello, F.; Schiavuta, P.; Suhling, K.; Anderson, H. L.; Cacialli, F. *Adv. Funct. Mater.* **2010**, *20*, 272−280. (b) Chen, Z.; Jiang, C.; Niu, Q.; Peng, J.; Cao, Y. *Org. Electron.* **2008**, *9*, 1002−1009.

(3) Collini1, E.; Wong, C. Y.; Wilk, K. E.; Curmi, P. M. G.; Brumer, P.; Scholes, G. D. *Nature* **2010**, *463*, 644−647.

(4) (a) Taranekar, P.; Huang, C.; Fulghum, T. M.; Baba, A.; Jiang, G.; Park, J.-Y.; Advincula, R. C. *Adv. Funct. Mater.* **2008**, *18*, 347−354. (b) Wu, C.; Zheng, Y.; Szymanski, C.; McNeill, J. *J. Phys. Chem. C* **2008**, *112*, 1772−1781. (c) Wu, C.; Bull, B.; Christensen, K.; McNeill, J. *Angew. Chem., Int. Ed.* **2009**, *48*, 2741−2745. (d) Satake, A.; Azuma, S.; Kuramochi, Y.; Hirota, S.; Kobuke, Y. *Chem.—Eur. J.* **2011**, *17*, 855−865. (e) Fujita, S.; Inagaki, S. *Chem. Mater.* **2008**, *20*, 891−908.

(5) (a) Patra, A.; Koenen, J.-M.; Scherf, U. *Chem. Commun.* **2011**, *47*, 9612−9614. (b) Kameta, N.; Ishikawa, K.; Masuda, M.; Asakawa, M.; Shimizu, T. *Chem. Mater.* **2012**, *24*, 209−228.

(6) Scholes, G. D.; Fleming, G. R.; Olaya-Castro, A.; van Grondelle, R. *Nat. Chem.* **2011**, *3*, 763−774.

(7) (a) Ajayaghosh, A.; Praveen, V. K.; Vijayakumar, C.; George, S. J. *Angew. Chem., Int. Ed.* **2007**, *46*, 6260−6265. (b) Abbel, R.; Grenier, C.; Pouderoijen, M. J.; Stouwdam, J. W.; Leclere, P. E. L. G.; Sijbesma, R. P.; Meijer, E. W.; Schenning, A. P. H. J. *J. Am. Chem. Soc.* **2009**, *131*, 833−843.

(8) Yeo, H.; Tanaka, K.; Chujo, Y. *J. Polym. Sci., Part A: Polym. Chem.* **2012**, *50*, 4433−4442.

(9) (a) Liu, S.-J.; Xu, W.-J.; Ma, T.-C.; Zhao, Q.; Fan, Q.-L.; Ling, Q.-D.; Huang, W. *Macromol. Rapid Commun.* **2010**, *31*, 629−6333. (b) Evans, N. R.; Devi, L. S.; Mak, C. S. K.; Watkins, S. E.; Pascu, S. I.; Köhler, A.; Friend, R. H.; Williams, C. K.; Holmes, A. B. *J. Am. Chem. Soc.* **2006**, *128*, 6647−6656. (c) Ego, C.; Marsitzky, D.; Becker, S.; Zhang, J.; Grimsdale, A. C.; Müllen, K.; MacKenzie, J. D.; Silva, C.; Friend, R. H. *J. Am. Chem. Soc.* **2003**, *125*, 437−443. (d) Chen, X.; Liao, J.-L.; Liang, Y.; Ahmed, M. O.; Tseng, H.-E.; Chen, S.-A. *J. Am. Chem. Soc.* **2003**, *125*, 636−637. (e) Wang, L.; Puodziukynaite, E.; Vary, R. P.; Grumstrup, E. M.; Walczak, R. M.; Zolotarskaya, O. Y.; Schanze, K. S.; Reynolds, J. R.; Papanikolas, J. M. *J. Phys. Chem. Lett.* **2012**, *3*, 2453−2457. (f) Buckley, A. R.; Rahn, M. D.; Hill, J.; Cabanillas-Gonzalez, J.; Fox, A. M.; Bradley, D. D. C. *Chem. Phys. Lett.* **2001**, *339*, 331−336. (g) Thivierge, C.; Loudet, A.; Burgess, K. *Macromolecules* **2011**, *44*, 4012−4015. (h) Wu, C.; Zheng, Y.; Szymanski, C.; McNeill, J. *J. Phys. Chem. C* **2008**, *112*, 1772−1781. (i) Becker, K.; Lupton, J. M. *J. Am. Chem. Soc.* **2006**, *128*, 6466−6479. (j) Russell, D. M.; Arias, A. C.; Friend, R. H.; Silva, C.; Ego, C.; Grimsdale, A. C.; Müllen, K. *Appl. Phys. Lett.* **2002**, *80*, 2204−2206. (k) Troshin, P. A.; Koeppe, R.; Susarova, D. K.; Polyakova, N. V.; Peregudov, A. S.; Razumov, V. F.; Sariciftci, N. S.; Lyubovskaya, R. N. *J. Mater. Chem.* **2009**, *19*, 7738−7744. (l) He, F.; Feng, F.; Wang, S.; Li, Y.; Zhu, D. *J. Mater. Chem.* **2007**, *17*, 3702−3707.

(10) Khan, A. L. T.; Sreearunothai, P.; Herz, L. M.; Banach, M. J.; Köhler, A. *Phys. Rev. B* **2004**, *69*, 085201.

(11) Hsu, F.-M.; Chien, C.-H.; Shu, C.-F.; Lai, C.-H.; Hsieh, C.-C.; Wang, K.-W.; Chou, P.-T. *Adv. Funct. Mater.* **2009**, *19*, 2834−2843.

(12) He, F.; Ren, X.; Shen, X.; Xu, Q.-H. *Macromolecules* **2011**, *44*, 5373−5380.

(13) (a) Jin, J.-K.; Kwon, S.-K.; Kim, Y.-H.; Shin, D.-C.; You, H.; Jung, H.-T. *Macromolecules* **2009**, *42*, 6339−6347. (b) Wu, F.-I.; Shih, P.-I.; Shu, C.-F. *Macromolecules* **2005**, *38*, 9028−9036.

(14) (a) Kubota, Y.; Uehara, J.; Funabiki, K.; Ebihara, M.; Matsui, M. *Tetrahedron Lett.* **2010**, *51*, 6195−6198. (b) Zhang, D.; Wen, Y.; Xiao, Y.; Yu, G.; Liu, Y.; Qian, X. *Chem. Commun.* **2008**, 4777−4779. (c) Hepp, A.; Ulrich, G.; Schmechel, R.; Von Seggern, H.; Ziessel, R. *Synth. Met.* **2004**, *146*, 11−15.

(15) (a) Ulrich, G.; Ziessel, R.; Harriman, A. *Angew. Chem., Int. Ed.* **2008**, *47*, 1184−1201. (b) Ziessel, R.; Ulrich, G.; Harriman, A. *New J. Chem.* **2007**, *31*, 496−501. (c) Bones, N.; Leen, V.; Dehaen, W. *Chem. Soc. Rev.* **2012**, *41*, 1130−1172.

(16) (a) Ziessel, R.; Harrimanb, A. *Chem. Commun.* **2011**, *47*, 611−631. (b) El-Khouly, M. E.; Amin, A. N.; Zandler, M. E.; Fukuzumi, S.; D'Souza, F. *Chem.—Eur. J.* **2012**, *18*, 5239−5247. (c) Gabe, Y.; Urano, Y.; Kikuchi, K.; Kojima, H.; Nagano, T. *J. Am. Chem. Soc.* **2004**, *126*, 3357−3367. (d) Mula, S.; Ray, A. K.; Banerjee, M.; Chaudhuri, T.; Dasgupta, K.; Chattopadhyay, S. *J. Org. Chem.* **2008**, *73*, 2146−2154.

(17) Klaerner, G.; Miller, R. D. *Macromolecules* **1998**, *31*, 2007−2009.

(18) Dieter, N. *Macromol. Rapid Commun.* **2001**, *22*, 1365−1385.

(19) Gu, Z.-Y.; Guo, D.-S.; Sun, M.; Liu, Y. *J. Org. Chem.* **2010**, *75*, 3600−3607.